

A simple “geometric” mapping function for the hydrostatic delay at radio frequencies and assessment of its performance

Ulrich Foelsche and Gottfried Kirchengast

Institute for Geophysics, Astrophysics, and Meteorology (IGAM), University of Graz, Graz, Austria

Received 4 July 2001; revised 29 January 2002; accepted 11 February 2002; published 30 May 2002.

[1] The hydrostatic mapping function, $m(\varepsilon)$, describes the dependence of the hydrostatic path delay on the elevation angle ε . We have developed a simple mapping function, where the only free parameter is an “effective height” of the atmosphere, H_{atm} , corresponding to about the first two scale heights above the surface. The value of $m(\varepsilon)$ is given by the ratio of the straight-line ray path length within height H_{atm} to height H_{atm} itself. We used simulated delays at GPS (Global Positioning System) frequencies derived from high resolution ECMWF (European Centre for Medium-Range Weather Forecasts) atmospheric analysis fields to assess the performance of the “geometric” mapping function relative to well established ones (the Davis, Niell, and Herring mapping functions, respectively). At elevations $>6^\circ$ the new mapping function generally exhibits, based on a single parameter, a performance comparable to or better than the other mapping functions. *INDEX TERMS*: 6904 Radio Science: Atmospheric propagation; 3360 Meteorology and Atmospheric Dynamics: Remote sensing; 1243 Geodesy and Gravity: Space geodetic surveys; 0365 Atmospheric Composition and Structure: Troposphere—composition and chemistry

1. Introduction

[2] For a plane parallel model of the Earth and the atmosphere (neglecting the curvature of the Earth and azimuthal variations within the atmosphere), the hydrostatic delay in an arbitrary slant direction, ΔL_h , is given by the cosecant law

$$\Delta L_h = \frac{1}{\sin(\varepsilon)} \Delta L_h^0 = \csc(\varepsilon) \Delta L_h^0, \quad (1)$$

where ε is the elevation angle of the radio source and ΔL_h^0 is the zenith hydrostatic delay. In general, ΔL_h can be written as

$$\Delta L_h = m(\varepsilon, \mathbf{p}) \Delta L_h^0. \quad (2)$$

[3] The function $m(\varepsilon, \mathbf{p})$, depending on the elevation angle ε and the vector \mathbf{p} (some parameterized representation of the atmospheric refractivity; [Davis *et al.*, 1985]), is usually called *mapping function*. By convention, the dependence on the vector \mathbf{p} is suppressed for the sake of simplicity.

2. The “Geometric” Mapping Function

[4] We introduce a simple “geometric” mapping function, where the only free parameter is an “effective height” of the atmosphere, H_{atm} , corresponding to about the first two scale heights above the surface. The value of $m(\varepsilon)$ is defined to be the

ratio of the slant straight-line ray path length within the “effective height”, S_{atm} , to the “effective height” itself

$$m(\varepsilon) = \frac{S_{atm}}{H_{atm}}. \quad (3)$$

[5] Equation (3) can alternatively be written in a form directly expressing the deviation from the simple cosecant law

$$m(\varepsilon) = \frac{1}{\sin(\varepsilon) \frac{S_{flat}}{S_{atm}}}, \quad (4)$$

where S_{flat} would be the ray path within H_{atm} in a flat (plane-parallel) atmosphere. The geometry is shown by Figure 1, which illustrates that S_{atm} can be determined by evaluation of the triangle formed by R_e , $R_e + H_{atm}$, and S_{atm} , where R_e is the radius of the Earth. Introducing the dimensionless ratio

$$\tilde{r} = \frac{R_e}{R_e + H_{atm}}, \quad (5)$$

the slant path length within H_{atm} can be expressed as

$$S_{atm} = (R_e + H_{atm}) [\cos(\arcsin(\tilde{r} \cos \varepsilon)) - \tilde{r} \sin \varepsilon]. \quad (6)$$

Inserting equation (6) into equation (3), the “geometric” mapping function can then be explicitly written as

$$m(\varepsilon) = \left(\frac{R_e}{H_{atm}} + 1 \right) [\cos(\arcsin(\tilde{r} \cos \varepsilon)) - \tilde{r} \sin \varepsilon]. \quad (7)$$

The free parameter H_{atm} should be set to ~ 15 km. For the present assessment it was set to 14.5 km at the Poles, linearly increasing to 15.5 km at the Equator. R_e was set to 6371 km.

3. Davis, Niell, and Herring Mapping Function

[6] The new mapping function was compared with the Davis, the Niell, and the Herring mapping functions, which are well established ones frequently encountered in literature.

[7] The Davis mapping function [Davis *et al.*, 1985], a modification of the continued fraction expansion introduced by Marini [1972], is given by

$$m(\varepsilon) = \frac{1}{\sin \varepsilon + \frac{a}{\tan \varepsilon + \frac{b}{\sin \varepsilon + c}}}. \quad (8)$$

where c is a constant while a and b are functions of surface temperature, surface total pressure, water vapor partial pressure at surface, height of the tropopause, and tropospheric temperature lapse rate, respectively.

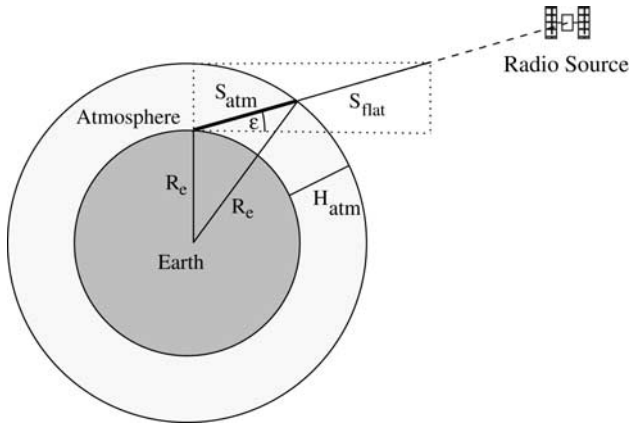


Figure 1. Schematic illustration of the construction of the “geometric” mapping function.

[8] The Niell mapping function [Niell, 1996] adopts a similar form, but does not depend on meteorology data

$$m(\varepsilon) = \frac{1 + \frac{a}{1 + \frac{b}{\sin \varepsilon + c}}}{\sin \varepsilon + \frac{a}{\sin \varepsilon + \frac{b}{\sin \varepsilon + c}}} \quad (9)$$

[9] At each latitude φ the coefficients a , b , and c are modeled as sinusoids in time, for example,

$$a(\varphi, doy) = a_{avg}(\varphi) - a_{ampl}(\varphi) \cos\left(2\pi \frac{doy - 28}{365.25}\right). \quad (10)$$

where the phase is defined by $doy = 28$ (corresponding to the winter extremum). In addition, a height correction is applied [see Niell, 1996 for details].

[10] The Herring mapping function has exactly the same form as the Niell mapping function. In the formulation used hereinafter [Herring, 1992], the coefficients depend on latitude, station height, and surface temperature, respectively.

4. Assessment Setup and Procedure

[11] High resolution (T213) analysis fields from the European Centre for Medium-Range Weather Forecasts (ECMWF) for

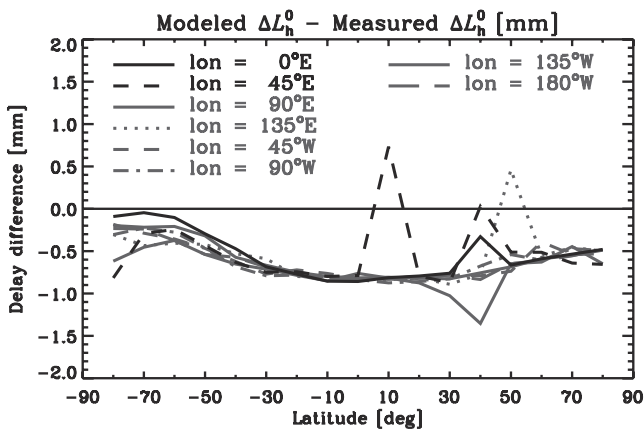


Figure 2. Difference between modeled (equation (12)) and “true” (realistically simulated) zenith hydrostatic delays for eight meridionally oriented chains of stations with 10° spacing for Sept. 15, 1999, 12UT (the absolute delay ΔL_h^0 at sea level is ~ 2.3 m).

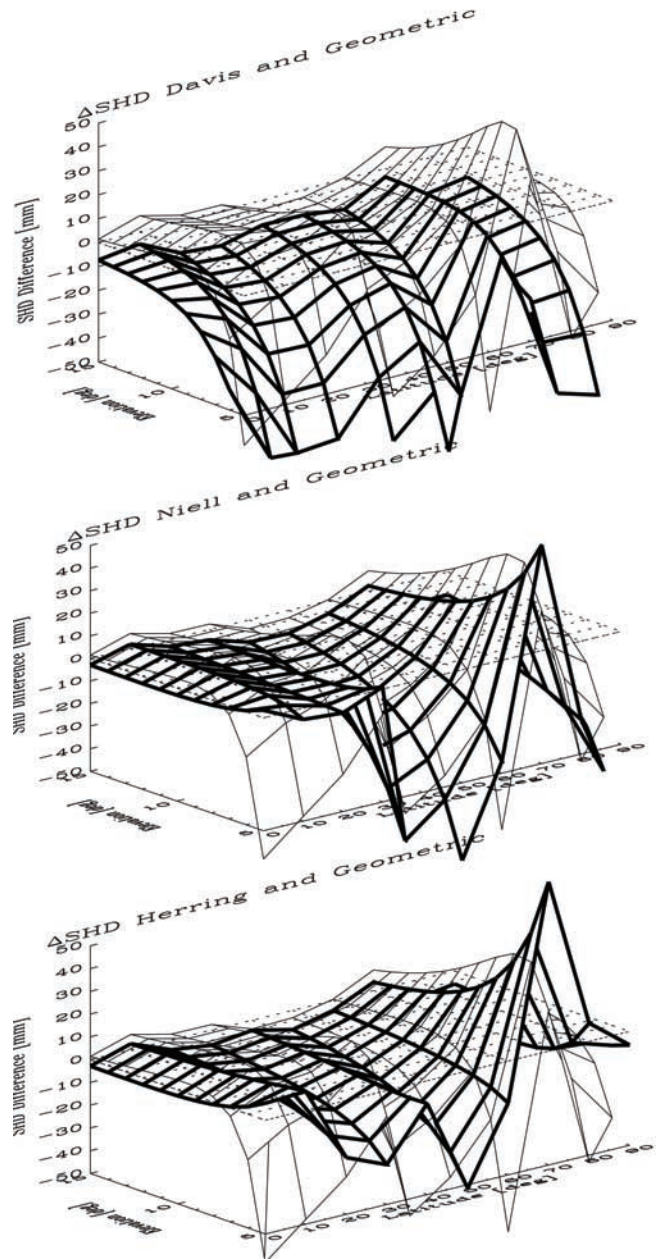


Figure 3. Differences between modeled and “true” slant hydrostatic delays for Sept. 15, 1999, 12UT, 45°E . The “geometric” mapping function (light-lined grid) is compared to the Davis (top), Niell (middle), and Herring (bottom) mapping functions (bold-lined grid), respectively.

September 15, 1999, 12UT (L50) and January 15, 2000, 12UT (L60), respectively, were used to generate realistic slant hydrostatic delays. We performed high-precision 3D ray tracing of slant rays to a synthetic GPS satellite for elevation angles between 5° and 15° (1° steps in the meridional plane, southward-looking). This was done for synthetic ground stations at latitudes between 0°N and 90°N (10° spacing) at eight different meridians (starting at 0°E , 45° spacing). The slant hydrostatic delay was calculated as

$$\Delta L_h = 10^{-6} \int_s N_{hyd}(s) ds + \Delta L_g = \frac{k_1}{10^6} \frac{R^*}{m_d} \int_s \rho(s) ds + \Delta L_g, \quad (11)$$

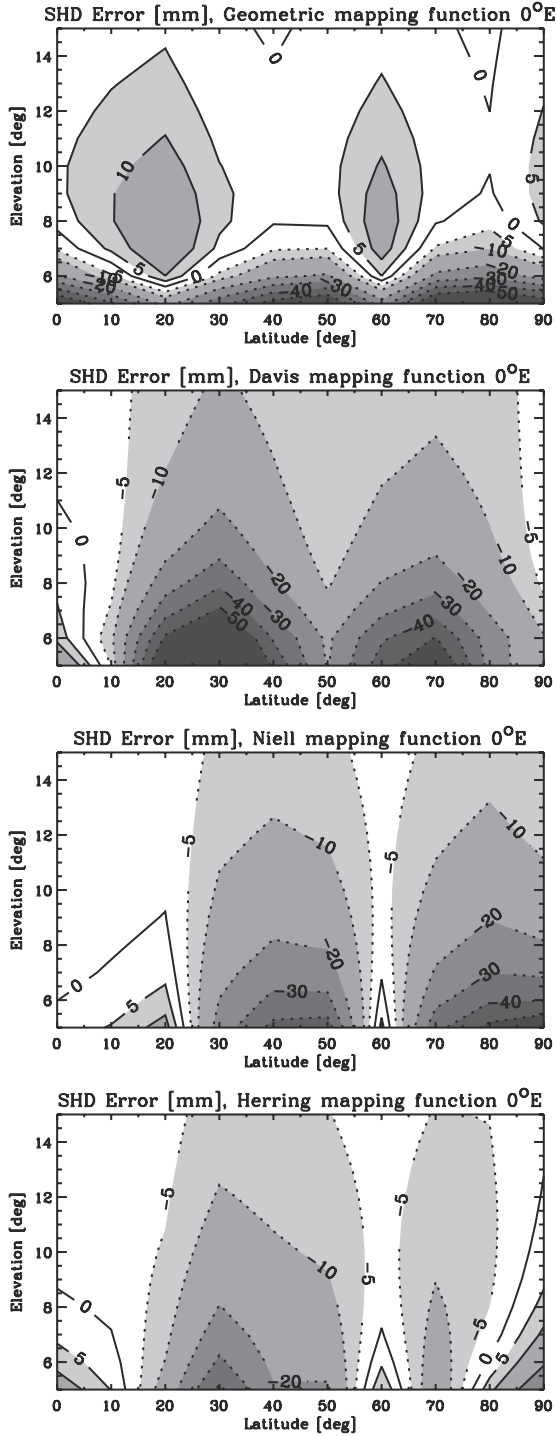


Figure 4. Differences between modeled and “true” slant hydrostatic delays for Sept. 15, 1999, 12UT, 0°E, using the “geometric” (top), Davis (upper middle), Niell (lower middle), and Herring (bottom) mapping function, respectively.

where N_{hyd} is the hydrostatic component of the refractivity N , ΔL_g is the “geometric delay” (the difference between the curved ray path S and the straight-line transmitter-receiver distance), $k_1 = 77.60$ K/hPa, R^* is the universal gas constant (8314.5 Jkmol $^{-1}$ K $^{-1}$), ρ is the total air density, and m_d is the molar mass of dry air (28.964 kg/kmol). A minor error is introduced as the bended ray path S is determined by the N_{hyd} -field and not by the complete N -field of the atmosphere.

[12] In zenith direction (indicated by the superscript “0”) the geometric delay vanishes and the hydrostatic delay can be estimated given the total surface pressure p_0

$$\Delta L_h^0 = \frac{k_1 R^*}{10^6 m_d} \int_0^\infty \rho(z) dz \cong \frac{k_1 R^*}{10^6 m_d g_m} \frac{p_0}{f(\varphi, H)}, \quad (12)$$

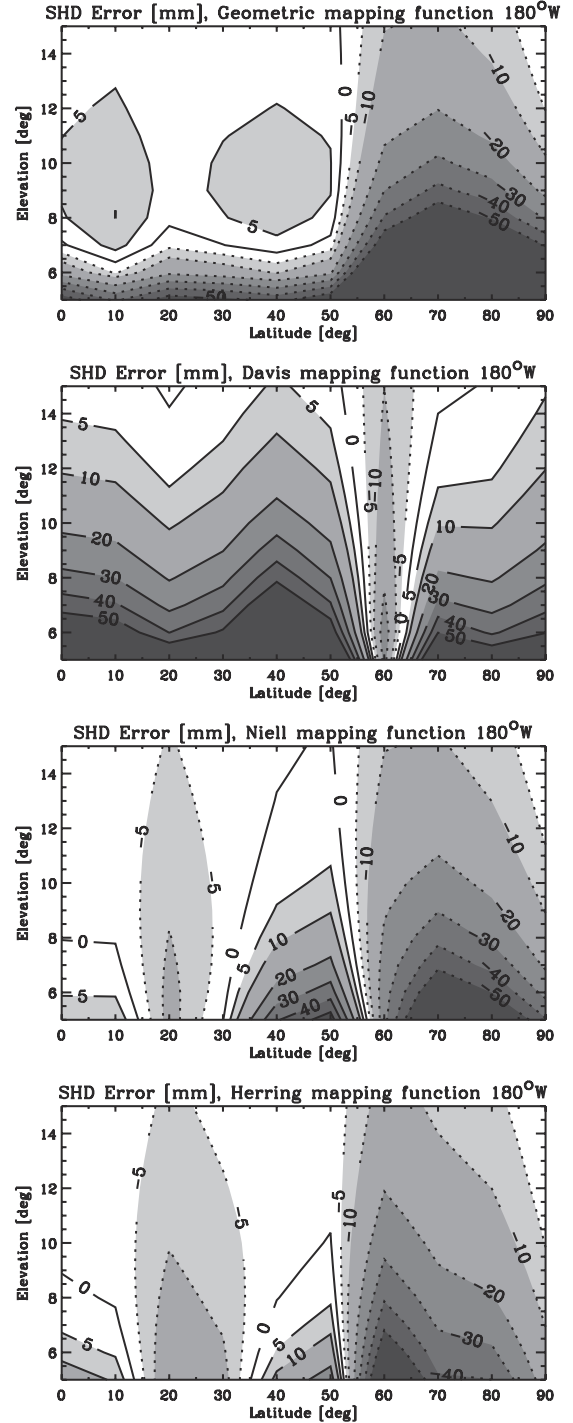


Figure 5. Differences between modeled and “true” slant hydrostatic delays for January 15, 2000, 12UT, 180°W, using the “geometric” (top), Davis (upper middle), Niell (lower middle), and Herring (bottom) mapping function, respectively.

with $g_m = 9.7837 \text{ m/s}^2$, and

$$f(\varphi, H) = 1 - 0.00265 \cos 2\varphi - 0.000285H, \quad (13)$$

where φ is the geographic latitude and H is the station height in [km] [Saastamoinen, 1972; Elgered, 1993].

[13] Zenith hydrostatic delays for each synthetic ground station were modeled using equation (12) and mapped onto the different ray paths using the four mapping functions described above. The results were compared to the simulated “true” slant hydrostatic delays obtained by the high-precision ray tracing.

5. Assessment Results

[14] In a prerequisite step we compared modeled and simulated hydrostatic delays at (near-)zenith elevations to check the performance of the ray tracer and the consistency of delays modeled via the right-hand side of equation (12) with simulated “true” delays based on ECMWF analysis fields. Simulated delays at 89° elevation in opposite directions about zenith showed a maximum absolute difference of 0.06 mm (standard deviation <0.02 mm), indicating that ray tracer errors are negligible. Differences between modeled and simulated zenith delays were computed for synthetic stations between 80°S and 80°N , for every meridian considered. Figure 2 shows that they exhibit, in general, a quite similar latitude dependence with a small negative bias of about 0.5 mm and largest deviations at low latitudes. With one exception (at 90°E , 40°N , Takla Makan desert), all differences are <1 mm, i.e., negligibly small for the present purpose.

[15] For the results shown in Figures 3 to 5, coefficients of the Niell mapping function were modeled following Niell [1996], those of the Davis *et al.* [1985] and the Herring [1992] mapping function were computed with “true” values of the meteorological parameters listed in section 3 (a most favorable choice, as “true” ones will never be available in practice). To put the results into perspective, note that the slant hydrostatic delay reaches typical values of ~ 23 m at 5° elevation.

[16] Figure 3 illustrates the general behavior of the different mapping functions (Sept. 15, 1999, 45°E , as an example) and provides a useful qualitative view on the performance. A complementary quantitative view is furnished by Figure 4 (Sept. 15, 1999, 0°E) and Figure 5 (January 15, 2000, 180°W), the latter showing results during the winter season.

[17] At elevations $<6^\circ$ the “geometric” mapping function shows a marked decrease in performance, but above this elevation the results are generally comparable to or even better than when using the other three mapping functions. Some exception in the present results is high-latitude winter accuracy (Figure 5, top), indicating a need to roughly model seasonal variation in H_{atm} .

6. Summary and Conclusions

[18] We have introduced a simple mapping function based on geometrical considerations. The only free parameter is an “effec-

tive height” of the atmosphere defined by about the first two pressure scale heights, which in this study was set to 14.5 km at the Poles, linearly increasing to 15.5 km at the Equator.

[19] Assessing the performance of the new “geometric” mapping function based on realistic ECMWF weather analysis fields, it was found to exhibit fairly good performance at $>6^\circ$ elevation. It shows promise to become an attractive alternative or complement to other mapping functions currently in use, especially when meteorology data are not available and when the elevation cut-off is set to $>6^\circ$, like in the field of GPS meteorology.

[20] A potential advantage of the new formulation is that the dependence on a single parameter would allow H_{atm} to be estimated from the GPS data themselves in a similar way as the zenith delays are estimated currently. Furthermore, when using a different “wet” H_{atm} value (of a few kms only), the formulation may also work as wet mapping function.

[21] An enhancement in the use of the “geometric” mapping function by introducing seasonal variations of the free parameter will further improve the performance. In a next step the new mapping function shall be tested with real GPS data.

[22] **Acknowledgments.** We are indebted to S. Syndergaard (Univ. of Arizona, Tucson, AZ, U.S.A) for his useful high-precision 3D ray tracer. We thank A. E. Niell and T. A. Herring (MIT, Boston, MA, U.S.A.) for providing valuable advice on the use of their mapping functions. The European Centre for Medium-Range Weather Forecasts (ECMWF, Reading, U.K.) kindly provided the atmospheric analysis fields used. The work was financially supported by the START research award of G. K. funded by the Austrian Ministry for Education, Science, and Culture and managed under Program No. Y103-CHE of the Austrian Science Fund.

References

- Davis, J. L., T. A. Herring, I. I. Shapiro, A. E. E. Rogers, and G. Elgered, Geodesy by radio interferometry: Effects of atmospheric modeling errors on estimation of baseline length, *Radio Sci.*, 20, 1593–1607, 1985.
- Elgered, G., Tropospheric radio path delay from ground-based microwave radiometry, in *Atmospheric remote sensing by microwave radiometry*, edited by M. A. Janssen, Wiley & Sons, NY, 215–258, 1993.
- Herring, T. A., Modelling atmospheric delays in the analysis of space geodetic data, in *Symposium on Refraction of Transatmospheric Signals in Geodesy*, Netherlands Geod. Commis. Ser. 36, edited by J. C. de Munck and T. A. Th. Spoelstra, 157–164, Ned. Comm. voor Geod., Delft, 1992.
- Marini, J. W., Correction of satellite tracking data for an arbitrary tropospheric profile, *Radio Sci.*, 7, 223–231, 1972.
- Niell, A. E., Global mapping functions for the atmosphere delay at radio wavelengths, *J. Geophys. Res.*, 101, 3227–3246, 1996.
- Saastamoinen, J., Introduction to practical computation of astronomical refraction, *Bulletin Géodésique*, 106, 383–397, 1972.

U. Foelsche and G. Kirchengast, Institute for Geophysics, Astro-physics, and Meteorology, University of Graz, Universitätsplatz 5, A-8010 Graz, Austria. (ulrich.foelsche@uni-graz.at; gottfried.kirchengast@uni-graz.at)